Pharm Res (2011) 28:2130–2139
DOI 10.1007/s11095-011-0440-7

RESEARCH PAPER

Cell-Penetrating Peptide-Modified Block Copolymer Micelles Promote Direct Brain Delivery via Intranasal Administration

Takanori Kanazawa • Hiroyuki Taki • Ko Tanaka • Yuuki Takashima • Hiroaki Okada

Received: 31 January 2011 / Accepted: 23 March 2011 / Published online: 16 April 2011

ABSTRACT

Purpose In order to develop non-invasive and effective nose-to-brain delivery of drugs, we synthesized Tat analog-modified methoxy poly(ethylene glycol) (MPEG)/poly(ε-caprolactone) (PCL) amphiphilic block copolymers through the ester bond.

Methods We evaluated the brain distribution of coumarin, acting as a model chemical, after intravenous or intranasal administration of MPEG-PCL. In addition, cellular uptake of coumarin by rat glioma cells transfected with coumarin-loaded MPEG-PCL or MPEG-PCL-Tat was determined. Finally, we determined the brain distribution and biodistribution after intranasal administration of coumarin-loaded MPEG-PCL-Tat.

Results The amount of coumarin in the brain after intranasal administration was significantly higher than that after intravenous administration. In addition, cellular uptake of coumarin using MPEG-PCL was the lowest, while cellular uptake of coumarin using Tat-modified MPEG-PCL (MPEG-PCL-Tat) was higher than that of MPEG-PCL. Therefore, the brain distribution of coumarin administered using MPEG-PCL-Tat was significantly greater than that using MPEG-PCL. Then, the coumarin distribution after MPEG-PCL-Tat administration in non-targeted tissues (lung, liver, heart, kidney and spleen) was lower than that after coumarin administration without nanomicelles.

Conclusion We have demonstrated that utilization of nano-sized micelles modified with Tat can facilitate direct intranasal brain delivery.

Takanori Kanazawa and Hiroyuki Taki contributed equally to this work.

T. Kanazawa (✉) • H. Taki • K. Tanaka • Y. Takashima • H. Okada
Laboratory of Pharmaceutics and Drug Delivery
Department of Pharmaceutical Science, School of Pharmacy
Tokyo University of Pharmacy and Life Sciences
1432-1 Horinouchi
Hachioji, Tokyo 192-0392, Japan
e-mail: kanazawa@toyaku.ac.jp

KEY WORDS biodistribution · brain tumors · cell penetrating peptide · intranasal brain delivery · micelles

INTRODUCTION

Despite the development of drugs that preferentially target tumor tissue without harming normal tissues, delivery of these drugs to brain tumors remains a major challenge because of the difficulty in penetrating the blood-brain barrier (BBB). Malignant gliomas are the most common primary tumors that occur in the human brain. The five-year survival rate for patients with glioblastoma (GBM), the most aggressive form of malignant glioma, is less than 5%, even with surgery followed by radiation therapy and chemotherapy (1). Clearly there is great need for new therapeutic strategies that will provide efficient drug delivery to brain tumors (2).

Investigations in animals and humans have shown that transport of exogenous materials directly from the nose to the brain is a potentially efficacious route for bypassing the BBB (3–5). Intranasal delivery provides a practical, noninvasive method for delivering therapeutic agents to the brain because of the unique anatomic connection provided by the olfactory and trigeminal nerves. These nerves connect the nasal mucosa and the CNS, allowing them to detect odors and other chemical stimuli (6,7). Intranasally administered drugs reach the parenchymal tissues of the brain and spinal cord and/or cerebrospinal fluid (CSF) within minutes using an extracellular route through perineural channels (2,8,9). In addition, intranasal delivery provides painless and convenient self-administration by patients, features that encourage its use for delivering therapeutic agents into the CNS (3–7). Furthermore, nanoparticles may offer improved nose-to-brain drug delivery since they are able to protect

the encapsulated drug from biological and/or chemical degradation and extracellular transport by p-GP efflux proteins. This would increase the availability of the drug to the CNS. Their small diameter potentially allows nanoparticles to be transported transcellularly through olfactory neurons to the brain via various endocytic pathways of sustentacular or neuronal cells in the olfactory membrane (5). In addition, we expect that surface modification of the nanoparticles, involving the addition of cell-penetrating peptides, could achieve penetration into the tumor cells in brain tumor tissue.

The cellular uptake of molecules can be enhanced by cell-penetrating peptides (CPP), which are cationic or amphiphilic molecules derived from various sources, including the human immunodeficiency virus Tat protein and *Drosophila antennapedia* homoprotein (10). A basic domain of Tat was previously shown to be the minimal sequence responsible for cellular and nuclear uptake, mediated by potential nuclear localization sequences in the 11-amino acid epitope YGRKKRRQRRR (11).

In the present study, we focused on brain delivery of drugs intranasally using block copolymers modified with or without Tat peptide synthesized in our previous study, which can form nano-sized micelles. Practically, in this study, to develop non-invasive and effective nose-to-brain delivery of drugs, we synthesized Tat analog-modified methoxy poly(ethylene glycol) (MPEG)/poly(ε-caprolactone) (PCL) amphiphilic block copolymers through the ester bond. The particle sizes of the formed particles before and after loading with coumarin, acting as a model chemical, were then determined. In addition, we evaluated the biodistribution or brain distribution of coumarin after intravenous or intranasal administration of MPEG-PCL. In addition, cellular uptake of coumarin by rat glioma (C6) cells transfected with coumarin-loaded MPEG-PCL or MPEG-PCL-Tat was determined. Finally, we also determined the brain distribution and biodistribution at various times after intranasal administration of coumarin-loaded MPEG-PCL-Tat.

MATERIALS AND METHODS

Materials, Cells and Animals

We purchased poly(ethylene glycol) (MPEG, $Mn = 2{,}000$) and coumarin-6 (coumarin) from Sigma-Aldrich Co. (Milwaukee, WI, USA). ε-caprolactone (PCL) was purchased from Tokyo Kasei (Tokyo, Japan) and camptotecin was from Wako Pure Chemical Industries, Ltd. (Osaka, Japan). C6 rat glioma (C6) cells were purchased from ATCC (USA). Cell culture media, F-12K nutrient mixture (F-12K), certified fetal bovine serum (FBS), penicillin/streptomycin stock solutions, and 0.25% Trypsin-EDTA were purchased from Invitrogen Co., USA. Seven-week-old Sprague-Dawley (SD) male rats were purchased from Japan SLC Inc. (Shizuoka, Japan). The rats were housed under standard conditions of temperature (22–24°C), humidity (40–60%), and 12-h light/dark-cycles with the light period stating at 08:00. Food and water were supplied *ad libitum*. All experiments with animals were carried out in accordance with a protocol approved by the Animal Care and Ethics Committee of Tokyo University of Pharmacy and Life Sciences (TUPLS).

Cell Culture and Inoculation of C6 Cells into the Left Side of the Brain

C6 cells were maintained in F-12K cell culture medium at 37°C and under 5% CO_2. F-12K media was supplemented with 10% FBS and 1% penicillin/streptomycin. Cells were seeded into culture flasks seven days before tumor implantation. For implantation, cells were harvested by trypsinization, washed once, and resuspended in F-12K medium. Then 1×10^6 C6 cells were intracranially inoculated into the left side of the brain of seven-week-old male SD rats.

Synthesis of MPEG-PCL Diblock Copolymer

MPEG-PCL diblock copolymer with a designed molecular weight of 4,000 was synthesized by ring-opening polymerization of ε-caprolactone in the absence of a catalyst, as described in our previous papers (12). Briefly, a predetermined amount of ε-caprolactone was added to a recovery flask containing MPEG and a small amount of hydrogen chloride 1.0*M* solution in diethyl ether (Sigma-Aldrich Co.). The recovery flask was then filled with N_2 gas, sealed off, and placed in an ice bath at 0°C for 3 h. At the end of the polymerization, the crude copolymers were precipitated in diethyl ether and centrifuged at 9,000 rpm for 3 min to remove any un-reacted monomer and oligomer. The white deposit was suspended in distilled water and dialyzed using a spectra/pore CE tube before being thoroughly freeze-dried. 1H NMR, FT-1R and gel permeation chromatography (GPC) were used to characterize the MPEG-PCL block copolymers according to our previous study (12).

Synthesis of the Tat Analog

The Tat-G analog, which consists of Gly-COOH added to the N-terminus of HIV-Tat (48–57) (Table I), was synthesized as CPP gene vector using the Fmoc-solid-phase peptide synthesis method with the ABI 433A peptide synthesizer (Applied Biosystems, USA) as previously reported (12–15). Both analogs were used after purification by reverse-phase HPLC. The molecular weights of the two

Table I Tat Analog Sequences

Name	Sequence
Tat-G (Tat) analog	Gly-Arg-Lys-Lys-Arg-Arg-Gln-Arg-Arg-Arg-Gly
Tat original	Gly-Arg-Lys-Lys-Arg-Arg-Gln-Arg-Arg-Arg

Tat analogs were determined by matrix-assisted laser desorption ionization time-of-flight mass spectrometry (MALDI-TOFMS): Tat-G analog, 1453.7

Synthesis of Tat-Conjugated MPEG-PCL Conjugated Through the Ester Bond

The hydroxyl group of the MPEG-PCL block copolymers was converted into a Tat analog through the ester bond. The Tat analog-conjugated MPEG-PCL was synthesized according to our previous report (12). Tat-G (0.02 mmol) and MPEG-PCL (0.02 mmol) were dissolved in dichloromethane, and then WSCI (0.02 mmol) and 4-dimethylaminopyridine (0.02 mmol) were added and reacted for 24 h. The reaction solution was then evaporated and dialyzed in distilled water using a dialysis tube (3,500 MW, Spectrum Laboratories, Inc., USA) for 24 h to remove the non-reacted Tat-G, and after freeze-drying, MPEG-PCL-conjugated-Tat conjugated through the ester bond (MPEG-PCL-Tat) was obtained.

Preparation of Blank or Comarin-6-Loaded Micelles

Blank MPEG-PCL micelles and MPEG-PCL-Tat micelles were prepared by the self assembly method. Coumarin was loaded into blank micelles by the w/o emulsion method (15). Briefly, different amounts of coumrin-6 inclusion dichloromethane solution were added to the micelle solution and ultrasonography applied for 3 min. After ultrasonic treatment, this w/o emulsion was evaporated to eliminate the dichloromethane. After adding appropriate quantities of distillated water, the suspension was filtered using a syringe filter (pore size: 0.8 μm) (ADVANTEC MSF, Inc.) to remove any insoluble coumarin. Finally, the coumarin-loaded micelles were obtained as a yellow powder after freeze drying.

Determination of the Physical Properties of Prepared Polymer Micelles

The mean particle size and zeta potential of the micelles were determined using a Zeta Potential/Particle Sizer NICOMP™ 380 ZLS (PSS. NICOMP PARTICLE SIZE SYSTEM, Santa Barbara, USA). The effect of freeze-drying on the particle size of the micelles was also evaluated.

Cellular Uptake of Various Coumarin Formulations

To study the kinetics of cellular uptake, various formulations of coumarin-loaded micelles (micelle concentration: 6.25 μg/mL) and coumarin solution were incubated with C6 cells for 1–4 h at 37°C (coumarin dose: 0.25 μg/mL). The mean particles sizes and zeta potential of coumarin-loaded MPEG-PCL or MPEG-PCL-Tat in this experiment are shown in Table III. After the incubation period, the medium was removed and the cells washed with PBS. An aliquot of lysis buffer was added to lyse the cells, and the fluorescence intensity of the coumarin in the buffer was determined using a microplate reader. The percent of uptake was calculated as the normalized concentration of internalized coumarin to the concentration of encapsulated coumarin being added.

Drug Disposition into the Brain after Intravenous or Intranasal Administration

This experiment was performed using a hydrophobic coumarin-encapsulated MPEG-PCL micelle system, with no Tat-analog modification and MPEG-PCL-Tat (micelle concentration: 5 mg/mL). The mean particles sizes and zeta potential of coumarin-loaded MPEG-PCL or MPEG-PCL-Tat in this experiment are shown in Table III. For intranasal administration, rats were anesthetized intraperitonealy with pentobarbital (50 mg/kg) and administered 50 μL of micelle suspension via a micropipette into each nostril (total 100 μL). Nose drops administered to animals lying on their backs resulted in consistent deposition in the olfactory epithelium. At 24 h (intravenous injection of MPEG-PCL), 1 h (intranasal injection of MPEG-PCL) or 4 h (intranasal injection of MPEG-PCL-Tat) post-treatment, brains were collected and homogenized at 12,000 rpm for 3 min using Polytron PT3100 (Kinematica, Inc., NY, USA). The coumarin fluorescence of each sample was observed by fluorescence microscopy (BZ-8100, Keyence).

Blood Concentration of Coumarin after Intaranasal or Intravenous Administration

Coumarin solution or coumarin-loaded MPEG-PCL micelles (micelle concentration: 5 mg/mL) were administered intranasally into healthy rats. The mean particles sizes and zeta potential of coumarin-loaded MPEG-PCL in this experiment are shown in Table III. As a negative control, coumarin solution was administrered intravenously into healthy rats. Blood was collected via the tail vein, kept in sampling tubes with heparin, and centrifuged to obtain plasma, after which dichloromethane was added to extract coumarin. Following shaking and centrifugation, the cou-

marin fluorescence in the supernatant was measured as described above.

Biodistribution and Drug Disposition into Organs in Tumor-Inoculated Rats

In the first experiment in this section we used different sized coumarin-loaded MPEG-PCL micelles (100 nm, 200 nm, 300 nm, 600 nm). At 14-day post transplantation, these micelles were administered intranasally (coumarin: 20 μg, micelle concentration: 5 mg/mL) into rats bearing C6 tumors. At 1 h post-treatment, the tissues of each organ (lung, heart, liver, spleen, kidney and brain) were collected and homogenized in lysis buffer at a volume-to-weight ratio of 4 mL lysis buffer per gram of each organ, and dichloromethane added to extract coumarin from each organ. After 15 min of shaking, the solutions were centrifuged at 14,000 rpm for 15 min to separate homogenate and dichloromethane. The coumarin fluorescence (excitation at 505 nm, emission at 540 nm) in the dichloromethane was measured using a microplate reader (Tecan Safire, Tecan Trading AG, Switzerland).

The second experiment examined differences in brain distribution of coumarin according to administration route. At 14 days after transplantation of C6 cells, coumarin-loaded MPEG-PCL was administered intravenously or intranasally at a dose equivalent of 20 μg coumarin (micelle concentration: 5 mg/mL). The mean particles sizes and zeta potential of coumarin-loaded MPEG-PCL in this experiment are shown in Table III. Rats were anesthetized and brain tissue obtained at 1 h after intranasal administration and at 24 h after intravenous administration. Brain tissue samples were homogenized and dichloromethane added to extract coumarin. Following shaking and centrifugation, coumarin fluorescence in the dichloromethane was measured as described above. In order to remove the original organ cell fluorescence at the same wavelength, the coumarin fluorescence of each organ and blood was measured without treatment with coumarin, and the results used to normalize the coumarin distribution results.

The third experiment examined the changes in the biodistribution of coumarin in the presence of Tat peptide-modified micelles. Coumarin-loaded MPEG-PCL and coumarin-loaded MPEG-PCL-Tat were administered intranasally (coumarin: 20 μg, micelle concentration: 5 mg/mL) into rats bearing C6 tumors intracranially. The mean particles sizes and zeta potential of coumarin-loaded MPEG-PCL or MPEG-PCL-Tat in this experiment are shown in Table III. At 1 h and 4 h post-treatment, the tissues of each organ were collected and homogenized, and dichloromethane added to extract coumarin from each organ. Following shaking and centrifugation, coumarin fluorescence in the dichloromethane was measured as described above.

Statistical Analysis

The data from the *in vitro* experiments express the mean ±S.D. The data from the *in vivo* experiments express the mean±S.E. Statistical analysis of the data was performed using an unpaired student's *t*-test for two groups. Statistical significance was defined as $*P<0.05$, $**P<0.01$, and $^{n.s.}P>0.05$.

RESULTS

Preparation and Characterization of MPEG-PCL and MPEG-PCL-Tat Micelles

MPEG-PCL block copolymers were synthesized by ring-opening polymerization of ε-CL in the presence of MPEG and characterized by ^{1}H NMR and GPC according to our previous study (12). The molecular weight of the MPEG-PCL block copolymers was 3,718 by GPC (calibrated with PEG standard) and 3,940 by the ^{1}H NMR spectrum. Conjugation of the Tat analog to MPEG-PCL through the ester bond was confirmed using the ninhydrin reaction, which becomes reddish violet upon reacting with the amino residue.

The particle size and zeta potential of MPEG-PCL and MPEG-PCL-Tat in distilled water are shown in Table II. Non-loaded MPEG-PCL is about 50 nm in size and has a slight negative charge in water. In contrast, non-loaded MPEG-PCL-Tat is about 30 nm in size and has a positive charge. In addition, as shown in Table III, coumarin-loaded MPEG-PCL is about 100 nm in size, with a loading efficiency of 70%, while coumarin-loaded MPEG-PCL-Tat is about 90 nm in size and has a loading efficiency of 90%.

Effect of Particle Size of MPEG-PCL Micelles after Intranasal Administration on Brain Distribution

The coumarin concentrations in the rat brain administered micelles loaded with coumarin show higher than that in non-injection rat brain (Fig. 1). Then, the coumarin

Table II Mean Diameter and Zeta Potential of Synthesized MPEG-PCL and MPEG-PCL-Tat

	Mean diameter (nm)	Zeta potential (mV)
MPEG-PCL	49 ± 3	−1.7 ± 0.8
MPEG-PCL-Tat	32 ± 6	7.3 ± 2.2

mean ± S.D., $n=3$

Table III Characterization of Coumarin-Loaded MPEG-PCL and MPEG-PCL-Tat

	Mean diameter (nm)	Zeta potential (mV)	Encapsulation (%)
MPEG-PCL	116 ± 13	−2.4 ± 0.6	74 ± 5
MPEG-PCL-Tat	73 ± 17	6.0 ± 1.3	86 ± 6

mean ± S.D., $n = 3$

concentrations in the rat brain administered 600 nm micelles loaded with coumarin show significantly lower than that in 100 nm administered rat brain.

The coumarin concentrations in the left side of the brain that inoculated with C6 tumor cells were higher than those in the right, non-inoculated side. On the other hand, the coumarin concentrations in the liver, heart, kidney, and spleen were lower than in the brain. In the spleen, the greater the particle size, the greater the detected coumarin concentrations.

Brain Distribution and Blood Concentration of Coumarin in Rats after Intravenous or Intranasal Administration

Figure 2a shows the brain distribution of coumarin in rats 1 h after intranasal or 24 h after intravenous MPEG-PCL nanomicelles administration. In the case of intravenously administered rats, the amount of coumarin in the left side of the brain (tumor-inoculated side) was significantly higher than that in the right side of the brain, indicating a passive tumor targeting effect was in action. In contrast, in the case of intranasally administered rats, the amount of coumarin

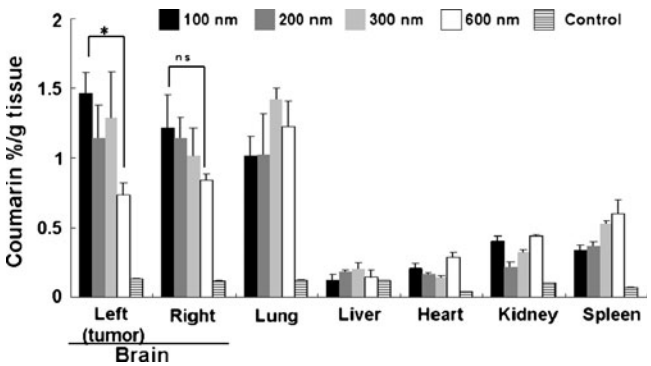

Fig. 1 Effect of particle size of coumarin-loaded MPEG-PCL micelles on biodistribution after intranasal administration to glioma C6 cells-bearing rats. Coumarin-loaded MPEG-PCL micells (dose: 20 μg as coumarin) having different sizes (100, 200, 300 and 600 nm) were administered by intranasal administration of C6 glioma tumor-inoculated rats (14 days post transplantation). Rats were sacrificed at 1 h after administration. Each *bar* represents the mean ± S.E., $n = 3$. n.s., not significant, $P > 0.05$; $^*P < 0.05$.

was similar in both sides of the brain, suggesting that the enhanced permeation and retention (EPR) effect was not connected with intranasal delivery. Furthermore, the amount of coumarin in the brain after intranasal administration was significantly higher than that after intravenous administration. Next, the coumarin fluorescence in the left brain homogenate after intravenous or intranasal administration of coumarin-loaded MPEG-PCL nanomicelles was observed using fluorescence microscopy (Fig. 2b). In the case of non-micelle-treated rats, no coumarin fluorescence was ever observed. On the other hand, coumarin fluorescence was observed in the coumarin-loaded MPEG-PCL nanomicelle-administered rats, with the fluorescence being significantly greater and stronger in the intranasally administered rats than in the intravenously administered rats.

Figure 3 shows the time-course of blood coumarin concentration in rats after intranasal or intravenous administration. The duration of blood circulation of coumarin in rats after intravenous administration was 48 h, which was significantly longer than that in the intranasally administered rats. In particular, we were only able to detect very low levels of coumarin in the blood of rats intranasally injected with coumarin-loaded MPEG-PCL micelles, indicating that drugs included within micelles can be intranasally delivered directly to the brain without leaking into the blood. However, coumarin was leaked into the blood circulation by intranasal administration of coumarin solution alone, soon after administration.

Cellular Uptake of MPEG-PCL and MPEG-PCL-Tat Micelles

The cellular uptake by C6 (rat glioma) cells transfected with coumarin solution, or coumarin-loaded MPEG-PCL or Tat-modified MPEG-PCL (MPEG-PCL-Tat) for 1–4 h is shown in Fig. 4. Cellular uptake of coumarin using MPEG-PCL was the lowest, while cellular uptake of coumarin using MPEG-PCL-Tat was higher than that of MPEG-PCL, but lower than that of coumarin solution. In the case of MPEG-PCL, the cellular uptake was not increased by transfection of any amount of coumarin-loaded micelles. In contrast, in the case of MPEG-PCL-Tat, the cellular uptake markedly increased according to the transfection with transfection times.

Brain Distribution of Coumarin-Loaded MPEG-PCL and MPEG-PCL-Tat Micelles after Intranasal Administration

The brain distribution in rats at 1 h and 4 h following intranasal administration of coumarin-loaded MPEG-PCL or MPEG-PCL-Tat is shown in Fig. 5a. At 1 h after

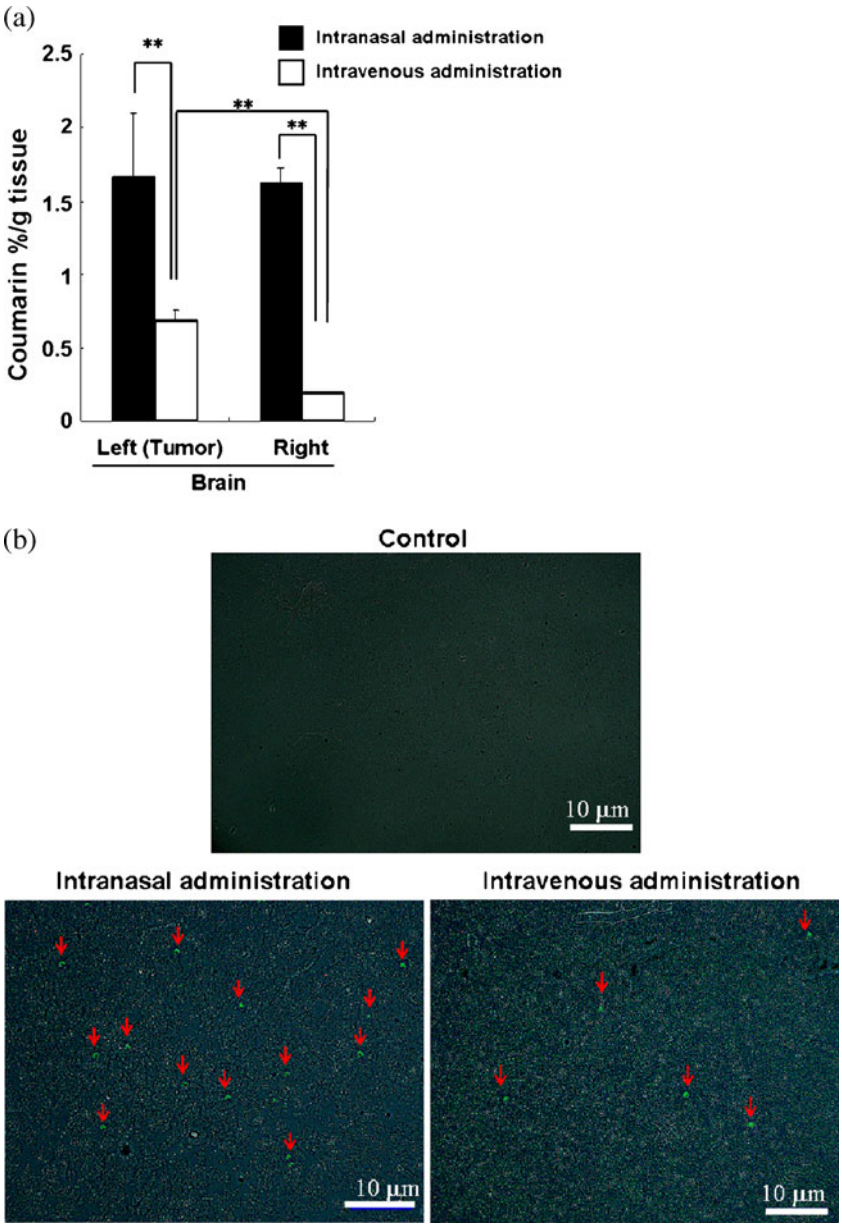

Fig. 2 Distribution of Coumarin in brain tissue after intravenous or intranasal administration of coumarin-loaded MPEG-PCL micelles. Rats were sacrificed at 1 h (intranasal) or 24 h (intravenous) post-injection of coumarin-loaded MPEG-PCL micells (Dose: 20 μg as coumarin). (**a**) Coumarin level in tumor-inoculated rats brain tissue. Each bar represents the mean ± S. E., $n=3$. $^{n.s}P>0.05$; $^{*}P<0.05$. (**b**) Observation of brain homogenates of healthy rats after intravenous or intranasal administration of coumarin-loaded MPEG-PCL micelles by fluorescence microscopy. Rats were sacrificed at 1 h (intranasal) or 24 h (intravenous) post-injection of coumarin-loaded MPEG-PCL micells (Dose: 20 μg as coumarin).

administration, there was no difference in the brain biodistribution of coumarin in rats intranasally administered MPEG-PCL or MPEG-PCL-Tat. However, at 4 h after administration, the brain distribution of coumarin in rats intranasally administered MPEG-PCL-Tat was significantly greater than that in rats administered MPEG-PCL. Then, in the case of MPEG-PCL-Tat, the coumarin distribution in the brain increased with time. Furthermore, the brain distribution of coumarin in rats at 4 h after intranasal administration with MPEG-PCL was lower than that at 1 h. We also observed coumarin fluorescence in homogenates of brain tissue obtained 4 h after intranasal administration of coumarin-loaded MPEG-PCL or MPEG-PCL-Tat nanomicelles using fluorescence microscopy. Similar to the results in Fig. 5a, coumarin fluorescence in brain homogenates from rats administered MPEG-PCL-Tat was greater than that in rats administered MPEG-PCL. Finally, we determined the biodistribution of coumarin in rats at 1 h or 4 h after intranasal administration of coumarin-loaded MPEG-PCL-Tat nanomicelles and at 1 h after intranasal administration of coumarin solution. As shown in Fig. 6, the coumarin distribution in non-targeted tissue (lung, liver, heart, kidney and spleen) administered with MPEG-PCL-Tat was smaller than that of coumarin solution and, in particular, was significantly smaller in lung, heart and kidney, strongly suggesting that there would probably be a decreased risk of side effects in these other tissues from intranasal MPEG-PCL-Tat administration.

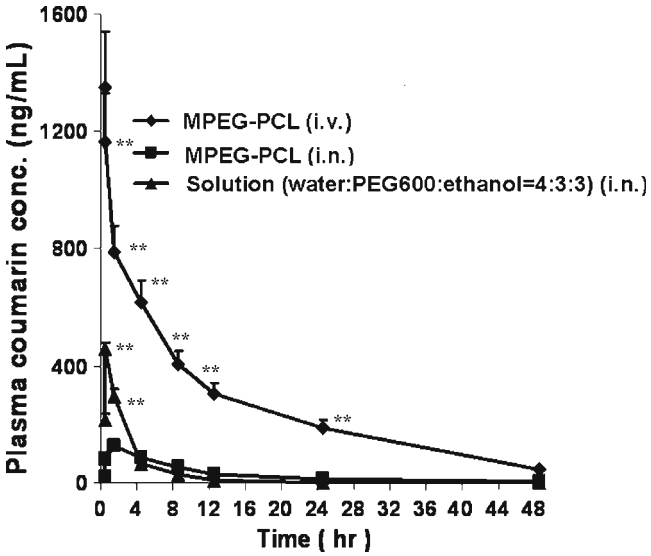

Fig. 3 Coumarin concentration in blood. Coumarin concentration in blood after administration of coumarin solution or coumarin-loaded MPEG-PCL (Dose: 20 μg as coumarin). Each *bar* represents the mean ± S.E., $n=3$. $^{**}P<0.01$ *versus* MPEG-PCL (i.n.).

DISCUSSION

Despite the development of drugs that preferentially target tumor tissue without harming normal tissues, delivery of these drugs to brain tumors remains a major challenge because of the difficulty in penetrating the blood-brain barrier (BBB). The five-year survival rate for patients with glioblastoma (GBM) is less than 5% even with surgery followed by radiation therapy and chemotherapy (1). Thus, there is great need for new therapeutic strategies that will provide efficient drug delivery into brain tumors (2).

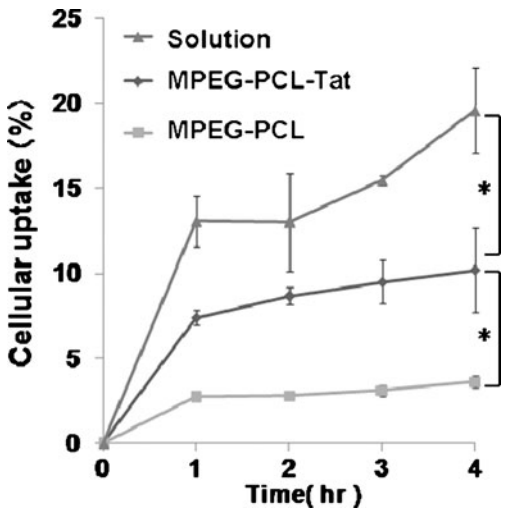

Fig. 4 Cellular uptake of MPEG-PCL or MPEG-PCL-Tat micelles in C6 glioma cells. Cells were incubated with micelles (coumarin dose: 0.25 μg/mL) for various hours (1–4 h). Each *bar* represents the mean ± S.D., $n=3$. $^{*}P<0.05$.

In this study, in order to develop a non-invasive and effective brain delivery system, we examined the brain distribution of drugs using a combination of intranasal administration and MPEG-PCL and Tat-modified MPEG-PCL. As shown in Table I, the particle size of the MPEG-PCL micelles was larger than that of the Tat analog-conjugated MPEG-PCL micelles; the zeta potential of MPEG-PCL showed a negative charge, whereas that of the Tat analog-conjugated MPEG-PCL (MPEG-PCL-Tat) showed a positive charge. Furthermore, coumarin-loaded MPEG-PCL and MPEG-PCL-Tat showed high loading efficiency of coumarin, which has a small particle size of around 100 nm and was used as a model material in this study (Table II). These findings suggest that synthesized MPEG-PCL and MPEG-PCL-Tat can form nanoparticles, possibly like a polymer micelle. In addition, regarding the structure of MPEG-PCL-Tat micelles in water, we speculate that the Tat analog is almost totally presented on the surface of the nanoparticles, since MPEG-PCL-Tat showed the positive charge of the Tat analog.

Next, we determined the coumarin biodistribution in brain tissue after intranasal administration of coumarin-loaded MPEG-PCL micelles (100 nm, 200 nm, 300 nm and 600 nm). As shown in Fig. 1, there is no effect of size between 100 nm, 200 nm and 300 nm on the uptake of coumarin nanoparticles into the left side or the right side of the brain. Furthermore, there does not appear to be a significant difference between the uptake of 200 nm, 300 nm and 600 nm coumarin nanoparticles. In contrast, coumarin concentration in the brain using intranasal MPEG-PCL nanoparticels with the smallest particle size (100 nm) was significantly higher than that with larger diameter (600 nm). In addition, a previous report has shown that particle size is an important property that is associated with the mucosal transport, and particles smaller than 100 nm, in general, have higher transport (16). Thus, the nanoparticles obtained with diameters of approximately 100 nm in this study can facilitate the nasal absorption and further uptake into CNS. Furthermore, it has been previously reported that a small diameter potentially allows nanoparticles to be transported transcellularly through olfactory neurons to the brain via various endocytic pathways of sustentacular or neuronal cells in the olfactory membrane (5–8). Therefore, these findings indicate that small nanoparticles are most useful for intranasal brain delivery. Furthermore, in general, the blood-brain barrier is disrupted in high-grade gliomas with all the components of the tumor blood vessels, i.e., endothelial cells, pericytes and the basement membrane, showing significant abnormalities (leaky vasculature) compared to normal cerebral vessels. In this experiment, although the blood-brain barrier of tumor cell inoculated side was expected to be disrupted, the significance difference between the coumarin concentra-

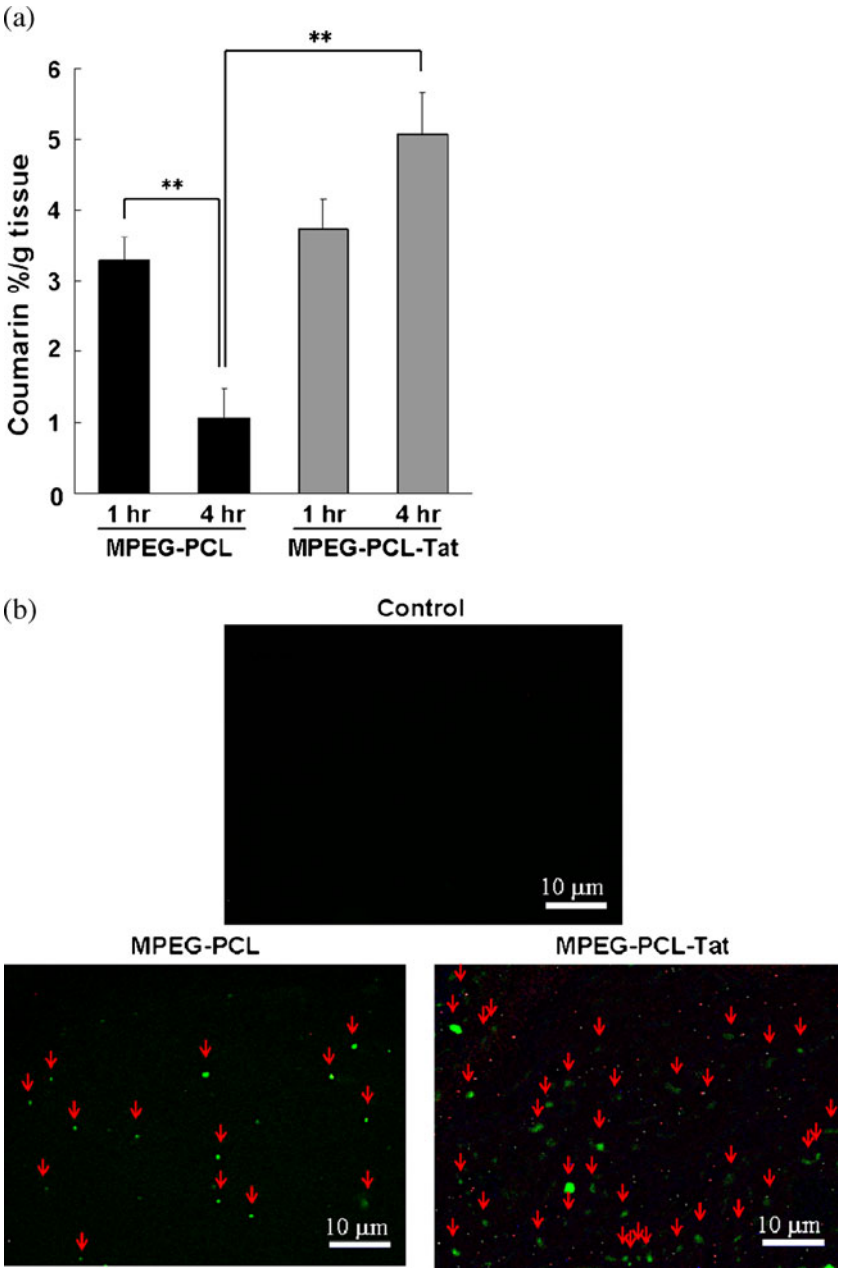

Fig. 5 Distribution of coumarin in brain tissue after intranasal administration of coumarin-loaded micelles. (**a**) Coumarin level in brain tissue. Rats were sacrificed at 1 h or 4 h post-injection of coumarin-loaded MPEG-PCL or MPEG-PCL-Tat micelles (dose: 20 μg as coumarin). Each *bar* represents the mean ± S.E., $n = 3$. *$P < 0.01$. (**b**) Observation of brain homogenates of rats at 4 h after intranasal administration of coumarin-loaded MPEG-PCL micelles by fluorescence microscopy.

tions in tumor and normal brain tissues was not observed (Fig. 1). On other hand, the coumarin concentrations in the liver, heart, kidney, and spleen were lower than in the brain, indicating that intranasal administration of drugs might be expected to decrease the risk of side effects in non-CNS tissues. However, in the case of the spleen, as particle size increased, coumarin concentration also increased, again suggesting that small-sized nanoparticles are the best carriers for nose-to-brain delivery.

We also compared the intravenous and intranasal MPEG-PCL nanomicelle administration routes for brain delivery efficiency (Fig. 2). The amount of coumarin in brain tissue after intranasal administration was significantly higher than that after intravenous administration, again proving intranasal delivery to be an effective method for brain targeting. In the intravenously administered rats, the amount of coumarin in the left side of the brain (tumor-inoculated side) was significantly higher than that in the right side of the brain, indicating a passive tumor targeting effect. In contrast, an EPR effect was not observed with intranasal delivery, suggesting that the nose-to-brain pathway is almost completely exclusive of blood vessels.

In addition, the duration of blood circulation of coumarin after intranasal administration was significantly

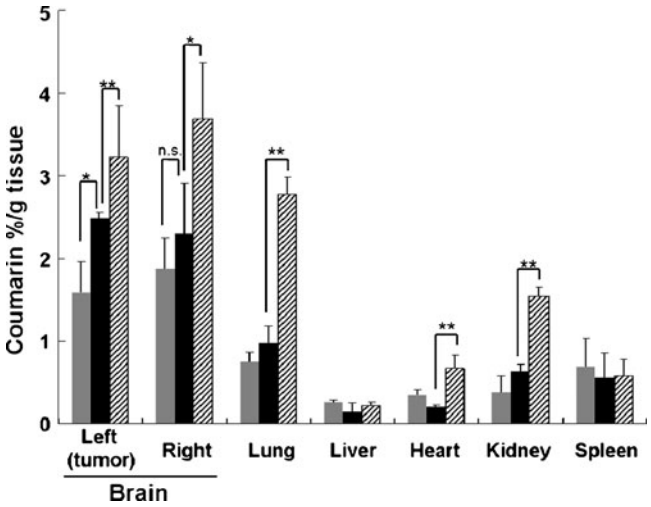

Fig. 6 Biodistribution of coumarin in rat after intranasal administration of coumarin-loaded MPEG-PCL-Tat micelles. Rats were sacrificed at 1 h ( ) or 4 h ( ) post-injection of coumarin-loaded MPEG-PCL-Tat micells or 1 h ( ) post-injection of coumarin solution (each dose: 20 μg as coumarin). Each *bar* represents the mean ± S.E., $n = 3$. $^{n.s.}P > 0.05$; $^{*}P < 0.05$; $^{**}P < 0.01$.

shorter than that after intravenous administration. In particular, we were only able to detect very low levels of coumarin in the blood of rats intranasally injected with coumarin-loaded MPEG-PCL micelles, indicating that drugs included within micelles can be intranasally delivered directly to the brain without leaking into blood. However, coumarin was leaked into the blood circulation by intranasal administration of coumarin solution alone, soon after administration. Thus, solution administration runs the risk of side effects in other tissues. These findings suggest that intranasal delivery of drugs into brain tissue using nano-sized micelles are more likely to be effective and less likely to produce side effects in non-CNS tissues.

We expected that modification of the surface using cell-penetrating peptides on the nanoparticles would achieve greater penetration into the tumor cells in brain tumor tissue. As shown in Fig. 5a, although there was no difference in the brain distribution of coumarin at 1 h after intranasal administration of MPEG-PCL or MPEG-PCL-Tat, at 4 h after intranasal administration, the brain distribution of coumarin administered using MPEG-PCL-Tat was significantly greater than that using MPEG-PCL. In addition, the coumarin fluorescence in brain tissue homogenates obtained 4 h after intranasal administration of MPEG-PCL-Tat was larger than that obtained with MPEG-PCL (Fig. 5b). This result was attributed to the difference in intracellular uptake ability between MPEG-PCL and MPEG-PCL-Tat. In fact, the CPP-modified MPEG-PCL, i.e., MPEG-PCL-Tat, promoted significantly larger intracellular uptake of coumarin in C6 tumor cells than MPEG-PCL (Fig. 4). In the case of MPEG-PCL, the brain distribution of coumarin at 4 h after administration was lower than that at 1 h, most likely because MPEG-PCL does not have the ability of intracellular permeation and is not able to penetrate brain cells. Therefore, the MPEG-PCL attached to the surface of cells had been perfused by CSF by 4 h after administration. In contrast, in the case of MPEG-PCL-Tat, the brain distribution of coumarin at 4 h after administration was greater than that at 1 h. As MPEG-PCL-Tat has the ability of intracellular penetration, MPEG-PCL-Tat was in the cells and thus MPEG-PCL-Tat might have not been perfused by CSF and then accumulated in the brain tissue by 4 h after administration.

Finally, we determined the biodistribution of coumarin at 1 h and 4 h after intranasal administration of coumarin-loaded MPEG-PCL-Tat nanomicelles. As shown in Fig. 6, the coumarin distribution after MPEG-PCL-Tat administration in non-targeted tissues (lung, liver, heart, kidney and spleen) was lower than that after administration of coumarin solution without nanomicelles. Furthermore, we are afraid that the potential side effects at the nasal cavity and CNS may be caused by delivering co-polymers into the brain. Thus, we will be conducting toxicological evaluation about nasal cavity and behavioral reaction during the course of the study.

CONCLUSION

The advantages of using intranasal delivery to bypass the BBB include rapid delivery to brain tissue, avoidance of hepatic first-pass drug metabolism, and elimination of the need for systemic delivery, thereby reducing the risk of unwanted systemic side effects. In addition, we have demonstrated that utilization of nano-sized micelles modified with CPPs can facilitate direct, intranasal brain delivery. In the near future, we will modify MPEG-PCL-Tat with an active sensor against tumor cells in an effort to establish a non-invasive and efficient glioblastoma treatment.

ACKNOWLEDGMENTS

We thank Mr. Shohei Suzuki and Mr. Fuminari Akiyama (School of Pharmacy, Tokyo University of Pharmacy and Life Sciences) for their excellent technical assistance. We are also grateful to Prof. Tsunehiko Fukuda, Ph.D. (Nagahama Institute of Bio-Science and Technology) for the peptide synthesis. This study was supported in part by a grant for private universities provided by the Promotion and Mutual Aid Corporation for Private Schools of Japan.

REFERENCES

1. CBTRUS, Central Brain Tumor Registry of the United States. Primary Brain Tumors in the United Atates: Statistical Report Tables, 1998–2002. 2005. Available from: http://www.cbtrus.org/2005-2006/tables/2006.table18-19.pdf.
2. Hashizume R, Ozawa T, Gryaznov SM, Bollen AW, Lamborn KR, Frey 2nd WH, *et al.* New therapeutic approach for brain tumors: intranasal delivery of telomerase inhibitor GRN163. Neuro Oncol. 2008;10:112–20.
3. Illum L. Transport of drugs from the nasal cavity to central nervous system. Eur J Pharm. 2000;11:1–18.
4. Illum L. Is nose-to-brain transport of drugs in man a reality? J Pharm Pharmacol. 2004;56:3–17.
5. Mistry A, Stolnik S, Illum L. Nanoparticles for direct nose-to-brain delivery of drugs. Int J Pharm. 2009;379:146–57.
6. Dhanda DS, Frey 2nd WH, Leopold D, Kompella UB. Approaches for drug deposition in the human olfactory epithelium. Drug Deliv Technol. 2005;5:64–72.
7. Thorne RG, Pronk GJ, Padmanabhan V, Frey 2nd WH. Delivery of insulin-like growth factor-1 to the rat brain and spinal cord along olfactory and trigeminal pathways following intranasal administration. Neuroscience. 2004;127:481–96.
8. Thorne RG, Frey 2nd WH. Delivery of neurotrophic factors to the central nervous system: pharmacokinetic considerations. Clin Pharmacokint. 2001;40:907–46.
9. Dhuria SV, Hanson LR, Frey 2nd WH. Intranasal delivery to the central nervous system: mechanism and experimental considerations. J Pharm Sci. 2010;99:1654–73.
10. Yang S, Coles DJ, Esposito A, Mitchell DJ, Toth I, Minchin RF. Cellular uptake of self-assembled cationic peptide-DNA complex: multifunctional role of the enhancer chloroquine. J Control Release. 2009;135:159–65.
11. Rajagopalan R, Xavier J, Rangaraj N, Rao NM, Gopal V. Recombinat fusion proteins TAT-Mu. Mu and Mu-Mu mediate efficient non viral gene delivery. J Gene Med. 2007;9:275–86.
12. Tanaka K, Kanazawa T, Shibata Y, Suda Y, Fukuda T, Takashima Y, *et al.* Development of cell-penetrating peptide-modified MPEG-PCL diblock copolymeric nanoparticles for systemic gene delivery. Int J Pharm. 2010;396:229–38.
13. Kanazawa T, Takashima Y, Hirayama S, Okada H. Effects on menstrual cycle on gene transfection through mouse vagina for DNA vaccine. Int J Pharm. 2008;360:164–70.
14. Uchida T, Kanazawa T, Takashima Y, Okada H. Development of an efficient transdermal delivery system of small interfering RNA using functional peptides, Tat and AT1002. Chem Pharm Bull. 2011;59:196–201.
15. Yokoyama M, Opanasopit P, Okano T, Kawano K, Maitani Y. Polymer design and incorporation methods for polymeric micelle carrier system containing water-insoluble anti-cancer agent camptothecin. 2004;12:373–84.
16. Brooking J, Davis SS, Illum L. Transport of nanoparticles across the rat nasal mucosa. J Drug Target. 2001;9:267–79.